Online parameter identification of synchronous machines using Kalman filter and recursive least squares

Erick F. Alves
Dept. of Electrical Power Engineering
NTNU
Trondheim, Norway
erick.f.alves@ntnu.no

Jonas K. Nøland
Dept. of Electrical Power Engineering
NTNU
Trondheim, Norway
jonas.k.noland@ntnu.no

Giancarlo Marafioti
Dept. of Mathematics and Cybernetics
SINTEF Digital
Trondheim, Norway
giancarlo.marafioti@sintef.no

Geir Mathisen
Dept. of Engineering Cybernetics
NTNU
Trondheim, Norway
geir.mathisen@ntnu.no

***Abstract*—This paper investigates and implements a procedure for parameter identification of salient pole synchronous machines that is based on previous knowledge about the equipment and can be used for condition monitoring, online assessment of the electrical power grid, and adaptive control. It uses a Kalman filter to handle noise and correct deviations in measurements caused by uncertainty of instruments or effects not included in the model. Then it applies a recursive least squares algorithm to identify parameters from the synchronous machine model. Despite being affected by saturation effects, the proposed procedure estimates 8 out of 13 parameters from the machine model with minor deviations from data sheet values and is largely insensitive to noise and load conditions.**

***Index Terms*—synchronous machines, parameter identification, condition monitoring**

I. Introduction

Synchronous generators are the bulk of power generation worldwide. In Norway, 95% of the electricity production comes from hydro power [1], in which the use of salient pole, synchronous generators is the norm. Therefore, the proper understanding of these devices is essential for planning, operation, and control of the power system [2]. Examples of tasks requiring adequate modeling and parametrization of synchronous machines (SMs) includes load flow analysis, state estimation, stability assessment and tuning of grid controls and protection settings. These tasks are important for transmission system operators or generation companies to operate their resources optimally and reliably.

Traditionally, SM parameters are calculated by manufacturers in the design phase using detailed information of the machine [3], [4] or by recursive methods such as finite-element analysis [5], [6]. Calculations are later validated during commissioning through acceptance or performance tests as described in IEEE and IEC Standards [7], [8]. These methods for parameter identification are well-proven and have been used for decades to operate the power system reliably. However, they have two major shortcomings.

The first is considering that many parameter values in the system equations are constants and do not vary with time. However, several effects may impact the values of SM parameters over time. For example, temperature and load conditions affects the air-gap length considerably [9]; field current level determines the saturation of the magnetic core [10]; aging influences material properties. The reason for adopting this restriction is simplifying the analysis of equations, which was done with limited computational resources when the theory for SMs was developed. However, the availability of powerful information and communication technologies today makes such simplifications neither reasonable nor justifiable.

The second shortcoming is requiring the machine to be in standstill or off-line for performing the majority of tests for parameter estimation. Since this means loss of income for generation companies, tests are only executed during commissioning or planned stops. This limits greatly the amount of data and possible operational conditions that can be measured. In Norway, the transmission system operator (Statnett) requires the registration of generators' parameters in SYSBAS for at least two weeks before commissioning, and an update with measured values after the machine starts commercial operation [11]. Yet, there is no requirement for periodical updates nor registration of distinct parameter values for different operational conditions.

Automated procedures for parameter identification of SMs were encouraged by the popularization of system identification techniques and their easy access in mathematical tools such as MATLAB© [12]. Methods are varied, but approaches can be summarized in analysis of transient data, such as short-

The authors thank SINTEF Digital for supporting this research.

circuit or load rejections; and frequency response tests, with injection of perturbations in standstill, off-line or on line operation. Successful examples of such automated procedures are extensive in the literature and are described in [13]–[23], among others.

This paper presents the following contributions: 1) the proposed procedure for parameter estimation can run with the machine online, and without taking it out of service, performing difficult and time-consuming tests or involving large perturbations; 2) the required input data are datasheet values and common measurements available in a power plant, i.e. there is no need to install additional transducers in the machine; 3) the algorithm is robust to noise and deviations in measurements caused by uncertainty of instruments or effects not included in the model.

Organization of the remaining sections are as following: sec. II introduces the SM equations, model and parameters; sec. III presents details about the Kalman filter used to estimate the states of the model and to filter out noise from outputs, and how this observer performs in several simulation cases and noise scenarios when compared to the SM model available in Simscape Power Systems (SPS); sec. IV describes the algorithm for parameter estimation, and how it performs in the same simulation cases and noise scenarios evaluated in sec. III; finally, sec. V presents conclusions, discussion, and ideas for further work.

II. Synchronous Machine Model

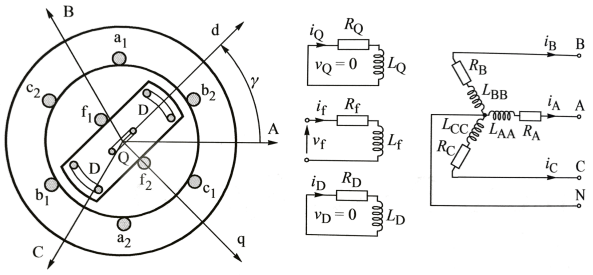

Fig. 1. The windings in the synchronous machine and their axes [24, p. 434]

This section presents the dynamic model of the SM used in this paper. Fig. 1 illustrates the SM windings, axes, input and output variables, while eq. (1) introduces its mathematical model in per-unit. The notation adopted follows the IEEE convention [25] and equations are based on [24, ch. 11].

$$\mathbf{v_{dq0fDQ}} = -\mathbf{R_{sm}}\mathbf{i_{dq0fDQ}} - \mathbf{L_{sm}}\frac{d}{dt}\mathbf{i_{dq0fDQ}} \qquad (1)$$

where $\mathbf{v_{dq0fDQ}} = \begin{bmatrix} v_d & v_q & v_0 & -v_f & 0 & 0 \end{bmatrix}^T$, $\mathbf{i_{dq0fDQ}} = \begin{bmatrix} i_d & i_q & i_0 & i_f & i_D & i_Q \end{bmatrix}^T$, and

$$\mathbf{R_{sm}} = \begin{bmatrix} R & \omega L_q & & & & \omega L_{aq} \\ -\omega L_d & R & & -\omega L_{ad} & -\omega L_{ad} & \\ & & R + 3R_N & & & \\ & & & R_f & & \\ & & & & R_D & \\ & & & & & R_Q \end{bmatrix}$$

$$\mathbf{L_{sm}} = \begin{bmatrix} L_d & & & L_{ad} & L_{ad} & \\ & L_q & & & & L_{aq} \\ & & L_0 + 3L_N & & & \\ L_{ad} & & & L_{ad} + l_f & L_{ad} & \\ L_{ad} & & & L_{ad} & L_{ad} + l_D & \\ & L_{aq} & & & & L_{aq} + l_Q \end{bmatrix}$$

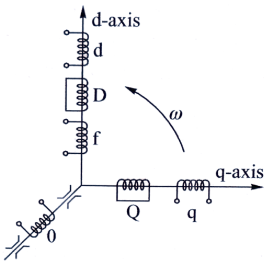

Fig. 2. Three sets of fictitious perpendicular windings representing the synchronous machine [24, p. 438]

In order to derive eq. (1), the following assumptions are made:

1) The three-phase stator winding is symmetrical, sinusoidally distributed and is wye/star connected;
2) The capacitance of all windings is neglected;
3) Each of the distributed windings is represented by a concentrated winding;
4) The change in the inductance of the stator windings due to rotor position is sinusoidal and does not contain higher harmonics;
5) Hysteresis losses are negligible but the influence of eddy currents is included in the model of the damper windings;
6) The magnetic circuits are linear (not saturated) and the inductance values do not depend on the current;
7) The electromagnetic effects of the three-phase stator armature windings shifted in space by 120° (a1, a2, b1, b2, c1, c2 in fig. 1) can be represented by three fictitious rotor windings all orthogonal to each other (d, q and 0 in fig. 2) by an isomorphic transformation, which is referred in the literature as the *dq0*-transformation [26];
8) Coefficients of the *dq0*-transformation matrix are chosen to make it orthogonal and power invariant;
9) The resistance of each of the stator phases is identical;
10) The effect of grounding is considered through an impedance on the zero-sequence voltage [27, ch. VIII].

A. State space representation

By inspection of eq. (1), it would be natural to assume $\mathbf{u} = \mathbf{v_{dq0fDQ}}$, $\mathbf{y} = \mathbf{x} = \mathbf{i_{dq0fDQ}}$, $\mathbf{A} = -\mathbf{L_{sm}}^{-1}\mathbf{R_{sm}}$, $\mathbf{B} = -\mathbf{L_{sm}}^{-1}$, $\mathbf{C} = \mathbf{I}$, $\mathbf{D} = \mathbf{0}$, and consider the state-space modeling done.

Nonetheless, for control purposes of a SM, it is more natural to assume $\mathbf{u} = \begin{bmatrix} i_d & i_q & i_0 & v_f & v_D & v_Q \end{bmatrix}^T$, since stator currents are defined by loads, field voltage is delivered by the excitation system and $v_D = v_Q = 0$. Thus,

$\mathbf{y} = \begin{bmatrix} v_d & v_q & v_0 & i_f & i_D & i_Q \end{bmatrix}^T$ and matrices $\mathbf{A}, \mathbf{B}, \mathbf{C}, \mathbf{D}$ must be redefined for a proper state space representation.

Assuming that, a state-space definition is easily achieved without major changes to the structure of eq. (1) by extending the model presented in fig. 1. Let suppose a balanced, star-connected load with resistance $R_{dl} = 10^4 Z_b$ is inserted at the ABC terminals of the machine, as shown in fig. 3. With that extension, the stator voltages in the (d, q, 0) reference frame can be expressed as $v_d = R_{dl}(i_d - i_{dt})$, $v_q = R_{dl}(i_q - i_{qt})$, $v_0 = R_{dl}(i_0 - i_{0t})$.

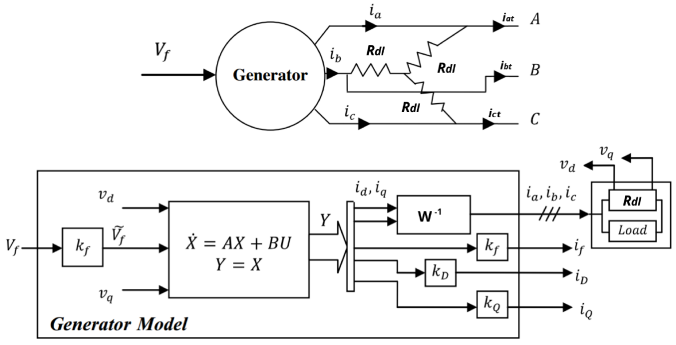

Fig. 3. Generator model with a dummy load, adapted from [28]

Notice that R_{dl} is considerably larger than the real load of the machine, therefore the difference between the terminal currents i_{at}, i_{bt}, i_{ct} and stator currents i_a, i_b, i_c is negligible. Re-arranging eq. (1) with these considerations, one obtains:

$$\mathbf{v_{dl}} = -\mathbf{R_{smdl}}\mathbf{i_{dq0fDQ}} - \mathbf{L_{sm}}\frac{d}{dt}\mathbf{i_{dq0fDQ}} \tag{2}$$

where $\mathbf{v_{dl}} = \begin{bmatrix} R_{dl}i_{dt} & R_{dl}i_{qt} & R_{dl}i_{0t} & v_f & 0 & 0 \end{bmatrix}^T$ and $\mathbf{R_{smdl}} =$

$$\begin{bmatrix} R+R_{dl} & \omega L_q & & & & \omega L_{aq} \\ -\omega L_d & R+R_{dl} & & -\omega L_{ad} & -\omega L_{ad} & \\ & & R+3R_N+R_{dl} & & & \\ & & & R_f & & \\ & & & & R_D & \\ & & & & & R_Q \end{bmatrix}$$

Hence, the following state space is defined:

$$\mathbf{u} = \mathbf{v_{dl}} \quad \mathbf{x} = \mathbf{i_{dq0fDQ}} \tag{3}$$

$$\mathbf{y} = \begin{bmatrix} v_d & v_q & v_0 & i_f & i_D & i_Q \end{bmatrix}^T \tag{4}$$

$$\mathbf{A} = -{\mathbf{L_{sm}}}^{-1}\mathbf{R_{smdl}} \tag{5}$$

$$\mathbf{B} = {\mathbf{L_{sm}}}^{-1} \tag{6}$$

$$\mathbf{C} = diag\begin{bmatrix} R_{dl} & R_{dl} & R_{dl} & 1 & 1 & 1 \end{bmatrix} \tag{7}$$

$$\mathbf{D} = diag\begin{bmatrix} -1 & -1 & -1 & 0 & 0 & 0 \end{bmatrix} \tag{8}$$

As the damper winding currents i_D, i_Q cannot be directly measured, an observer must be implemented. The transfer function for the observer for damper windings (ODW) currents is derived by applying the Laplace transform to rows 5 and 6 of eq. (2), and manipulating the expressions further to obtain:

$$i_D = -\frac{sL_{ad}}{s(L_{ad}+l_D)+R_D}(i_d + i_f) \tag{9}$$

$$i_Q = -\frac{sL_{aq}}{s(L_{aq}+l_Q)+R_Q}i_q \tag{10}$$

III. Optimal observer with Kalman filter

Good parameter estimation of synchronous machines requires accurate and precise measurement of inputs and outputs from eq. (1). However, some practical challenges must be addressed:

- Damper winding currents cannot be measured directly;
- Measurements are extremely affected by noise due to the high level of electromagnetic interference in a power plant;
- Voltage and current measurements may come from several independent sources, such as potential and current transformers for measurement or protection, each of them having different precision and accuracy values.

In the proposed procedure, measurements are filtered and corrected by a Kalman filter (KF) using prior knowledge about the synchronous machine model and its parameters. In addition to the state-space definition, three additional matrices must be specified to define a KF [29, chap. 5]:

- $\mathbf{Q}$, a SxS matrix (S=number of states) in which the diagonal elements represents the noise covariance of the states, also called process noise covariance matrix;
- $\mathbf{R}$, a YxY matrix (Y=number of outputs) in which the diagonal elements represents the noise covariance of the outputs, also called measurement noise covariance matrix;
- $\mathbf{N}$, a SxY matrix in which the elements represents the noise cross-covariance between states and outputs, also called process and measurement noise cross-covariance matrix.

It is assumed $\mathbf{N} = \mathbf{0}$, i.e. there is no cross-correlation between the noise of states and outputs. The other matrices are defined as $\mathbf{Q} = diag\begin{bmatrix} 0.05 & 0.05 & 0.05 & 0.05 & 0.03 & 0.03 \end{bmatrix}$ and $\mathbf{R} = diag\begin{bmatrix} 0.05 & 0.05 & 0.05 & 0.05 & 0.05 & 0.05 \end{bmatrix}$. Notice that the choice of diagonal $\mathbf{Q}$ and $\mathbf{R}$ matrices represents a naive assumption that state and output changes are uncorrelated.

These values produce robust results in several load conditions with and without noise or saturation, as seen in secs. III-A and IV-A. However, fine tuning might be required in the field for better performance, according to the level of noise, measurement accuracy and precision of each power plant. In practice, these values are also affected by the variance of $\mathbf{A}, \mathbf{B}, \mathbf{C}, \mathbf{D}$ elements.

A. Model validation

A simulation in MATLAB/Simulink is implemented to validate the KF and the ODW. It contains a load connected to a SM model in pu from the SPS, which is used as benchmark.

TABLE I
PARAMETERS OF THE SALIENT-POLE SYNCHRONOUS MACHINE USED AS BENCHMARK

Parameter	Value	Parameter	Value
S_n	555 MVA	L_{ad}	1.66 pu
U_n	24 kV	L_{aq}	1.61 pu
f_n	60 Hz	l_D	0.1713 pu
I_{fn}	1300 A	l_Q	0.7252 pu
p	1 pair	R_f	0.0006 pu
R	0.003 pu	l_f	0.165 pu
l_l	0.15 pu		

Parameters of a real synchronous machine are taken from examples 3.1, 3.2 and 8.1 of [2, p. 91,102,345] and listed in table I. Saturation effects in the SPS SM model is included.

The rotor speed is assumed constant, i.e. the prime mover and its turbine governor are not modeled because the mechanical dynamics are much slower than the electrical and have little influence in the results. The field voltage is provided by an DC1C type excitation system as described in [30]. The choice of parameters for the automatic voltage regulator (AVR) gives a fast and stable response, without overshoot in the terminal voltage. However, they are not optimized and a power system stabilizer is not included, as detailed modeling and optimization of the excitation system will have little influence in the results.

The outputs of the SM, i.e. stator and field measurements $v_a, v_b, v_c, v_f, i_a, i_b, i_c, i_f$ together with the rotor mechanical angle γ, are fed into a measurement block that: 1) adds band-limited white noise and re-samples measurements into a lower sample frequency (400 Hz) in order to make them more realistic; 2) applies the *dq0*-transformation and converts the values to *per-unit*. Finally, the output of the measurement block is fed into the proposed ODW and KF.

The simulation runs with the following load conditions, where P represent the active power, Q the reactive power and the per-unit base is given in table I:

- Case 1: P = 0 pu, Q = 0 pu (no load);
- Case 2: P = 0.5 pu, Q = 0.5 pu;
- Case 3: P = 0.5 pu, Q = -0.5 pu;
- Case 4: P = 0.9 pu, Q = 0.4359 pu (rated load).

In all cases, the simulation starts at rated stator voltage. In order to observe transient behavior, a step of +5% is applied to the reference of the AVR at time $t = 17$ seconds. The initial states of the SM are calculated using the Machine Initialization tool from SPS in order to avoid loss of synchronism. However, initial states of ODW and KF are all zero, so it is necessary some seconds of simulation to achieve steady state. This also demonstrates the KF robustness to wrong initial conditions and large transients.

In addition, the following noise power density (N_p) scenarios are used for each simulation case: no noise $N_p = 0$, standard noise $N_p = 10^{-10}$ W/Hz, high noise $N_p = 10^{-9}$ W/Hz.

Table II benchmarks the proposed KF against the SPS SM by presenting the *goodness of fit* between the two models using the normalized mean square error (NMSE) as cost function. The latter is defined as:

$$NMSE = 1 - \frac{\|x_{ref} - x\|^2}{\|x_{ref} - mean(x_{ref})\|^2} \tag{11}$$

where $\|$ indicates the Euclidean or L^2 norm of a vector. NMSE costs vary between $-\infty$ (bad fit) to 1 (perfect fit).

Below follow some remarks about the results:

- NMSE of v_d and i_Q are very low in case 1 (no load) because their values tend to zero and, since the noise power is constant, the signal-to-noise ratio (SNR) is extremely low. This makes NMSE measurement not relevant for these cases, so they are excluded from the standard deviation (std dev) calculation.
- The mean correlation between KF and SPS for all variables except i_D is close to unity in the no noise scenario. This shows the two models are nearly equivalent;
- The KF does not compensate saturation effects for i_D. Saturation changes the value of L_{ad}, which is the main component of the zero and pole of i_D transfer function in the ODW, as shown in eq. (9). The variation of L_{ad} makes the state transition function non linear, and improper for a KF to handle;
- The KF effectively compensates saturation effects for v_q, i_f in the no and standard noise scenarios. As expected, performance is degraded in the high noise scenario due to a lower SNR;
- The low standard deviation between all cases indicates the correlation is not sensitive to the load conditions;
- Also in the standard noise scenario, correlation between KF and SPS is relatively close to unity and with small standard deviation, expect for i_D;
- As expected, the performance of ODW with saturation and noise is degraded, but it is fairly improved by the KF;
- The performance of the KF gets better in the high noise scenario when the load increases, because the SNR also improves;

IV. ALGORITHM FOR PARAMETER ESTIMATION

Eq. (1) shows that, in matricial form, a synchronous machine can be reduced to an impedance with a resistive part $\mathbf{R_{sm}}$ and an inductive part $\mathbf{L_{sm}}$. Given this model structure and the set of process signal $\mathbf{v_{dq0fDQ}}, \mathbf{i_{dq0fDQ}}$, the goal is to estimate the elements of matrices $\mathbf{Rsm}, \mathbf{Lsm}$. So, the only piece left is defining an approximation or error criterion.

The literature has some accounts of error criteria for parameter identification of synchronous machines, such as extended Kalman filter (EKF) [31], Levenberg–Marquardt algorithm [14], recursive least squares (RLS) [15], [16], Prony method [17], among others.

In this paper, the error criterion used is the RLS. The main reasons for this choice are: 1) RLS is readily available in the System Identification Toolbox of Simulink; 2) near real-time execution is possible with RLS due to its recursive nature and low computational effort when compared to other methods.

TABLE II
NMSE VALUES FOR ALL SIMULATION CASES AND NOISE SCENARIOS WITH SATURATION

Variable	Case 1	Case 2	Case 3	Case 4	Mean	Std dev
No noise scenario						
v_d KF	1.000	1.000	1.000	1.000	1.000	9.93e-10
v_q KF	1.000	1.000	1.000	1.000	1.000	2.39e-09
i_f KF	1.000	1.000	1.000	1.000	1.000	8.56e-06
i_D ODW	0.609	0.637	0.997	0.975	0.804	2.10e-01
i_D KF	0.612	0.620	0.995	0.964	0.798	2.11e-01
i_Q ODW	1.000	1.000	1.000	1.000	1.000	6.43e-08
i_Q KF	-437	0.995	1.000	0.999	0.998	2.66e-03
Standard noise scenario						
v_d KF	-489	0.954	0.996	0.984	0.978	2.18e-02
v_q KF	0.996	0.994	0.988	0.988	0.991	4.13e-03
i_f KF	0.999	1.000	0.995	0.999	0.998	2.34e-03
i_D ODW	0.448	0.431	0.907	0.753	0.635	2.34e-01
i_D KF	0.559	0.551	0.965	0.889	0.741	2.17e-01
i_Q ODW	-5263	0.859	0.991	0.932	0.927	6.63e-02
i_Q KF	-2305	0.945	0.997	0.975	0.972	2.59e-02
High noise scenario						
v_d KF	-4890	0.540	0.963	0.844	0.782	2.18e-01
v_q KF	0.961	0.937	0.884	0.876	0.915	4.13e-02
i_f KF	0.988	0.995	0.946	0.994	0.981	2.33e-02
i_D ODW	-1.005	-1.437	0.096	-1.253	-0.900	6.87e-01
i_D KF	0.066	-0.080	0.692	0.211	0.222	3.35e-01
i_Q ODW	-52633	-0.414	0.909	0.321	0.272	6.63e-01
i_Q KF	-19133	0.496	0.968	0.759	0.741	2.37e-01

This is essential when considering direct implementation in an existing intelligent electronic devices (IEDs) or phasor measurement units (PMUs); 3) benchmarks exist in the literature for comparison of results.

Considering simultaneous estimation of the 13 parameters of the synchronous machine with RLS estimation generates poor results [16], simplifications are required. Thus, steady-state is assumed, i.e. $\frac{d}{dt}\mathbf{i_{dq0fDQ}} = \mathbf{0}$. Therefore, parameters from matrix $\mathbf{R_{sm}}$ can be estimated using RLS, but not $\mathbf{L_{sm}}$. However, notice that 4 out of 8 parameters from $\mathbf{L_{sm}}$ are also present in $\mathbf{R_{sm}}$.

Another practical assumption is the stator resistance R should not be estimated in rows 1 and 2 of matrix $\mathbf{R_{smdl}}$. The arguments for this assumption are: 1) R is not used for the calculation of any standard parameter of the SM [2, section 4.2]; 2) R in pu is usually two to three orders of magnitude smaller than other parameters in these rows ($\omega L_d, \omega L_{ad}, \omega L_q, \omega L_{aq}$), what makes a reliable estimation challenging [32].

Considering all assumptions above, eq. (1) can be re-arranged into:

$$\mathbf{v_{RLS}} = -\mathbf{R_{RLS}}\mathbf{i_{dq0fDQ}} \tag{12}$$

where $\mathbf{v_{RLS}} = \begin{bmatrix} v_d - Ri_d & v_q - Ri_q & v_0 & -v_f & 0 & 0 \end{bmatrix}^T$ and

$$\mathbf{R_{RLS}} = \begin{bmatrix} & \omega L_q & & & & \omega L_{aq} \\ -\omega L_d & & & -\omega L_{ad} & -\omega L_{ad} & \\ & & R + 3R_N & & & \\ & & & R_f & & \\ & & & & R_D & \\ & & & & & R_Q \end{bmatrix}$$

Notice that in $\mathbf{v_{RLS}}$, the stator voltages v_d, v_q are compensated with the voltage drops in the stator resistance Ri_d, Ri_q. Also $R + 3R_N$ is estimated in the third row. In summary, eq. (1) is only re-arranged to avoid the estimation of R individually, as this parameter is not useful to calculate the standard parameters (table III). Moreover, its use for condition monitoring is compromised because it cannot be estimated reliably.

The leakage reactances l_f, l_D, l_Q are not estimated by the RLS algorithm. Hence, they are assumed constants for calculation of standard parameters. This is a reasonable assumption considering they represent a flux path through air and are less affected by saturation or temperature changes.

Finally, the steady-state condition is detected in run-time by monitoring that the damper windings currents are below a certain level, as those flow only in transient conditions. Fine tuning in the field of this threshold might be required for better performance, according to the noise level, measurement accuracy and precision of each power plant.

TABLE III
STANDARD PARAMETERS OF A SALIENT-POLE SYNCHRONOUS MACHINE AS DEFINED IN [2, SECTION 4.2]

Parameter	Definition
X_d	$\omega(L_{ad} + l_l)$
T'_{d0}	$\frac{L_{ad} + l_f}{R_f} + \frac{L_{ad} + l_D}{R_D}$
T'_d	$\frac{1}{R_f}(l_f + \frac{L_{ad} l_l}{L_{ad} + l_l}) + \frac{1}{R_D}(l_D + \frac{L_{ad} l_l}{L_{ad} + l_l})$
T''_{d0}	$\frac{1}{T'_{d0} R_f R_D}(l_D + \frac{L_{ad} l_f}{L_{ad} + l_f})(L_{ad} + l_f)$
T''_d	$\frac{1}{T'_d R_f R_D}(l_D + \frac{L_{ad} l_l l_f}{L_{ad} l_l + L_{ad} l_f + l_l l_f})(l_f + \frac{L_{ad} l_l}{L_{ad} + l_l})$
X'_d	$X_d \frac{T'_d}{T'_{d0}}$
X''_d	$X'_d \frac{T''_d}{T''_{d0}}$
X_q	$\omega(L_{aq} + l_l)$
T''_{q0}	$\frac{(L_{aq} + l_Q)}{R_Q}$
X''_q	$\omega(l_l + \frac{L_{aq} l_Q}{L_{aq} + l_Q})$

A. Parameter estimation validation

For validation of the parameter estimator, the simulation file runs at exactly the same conditions as described in sec. III-A.

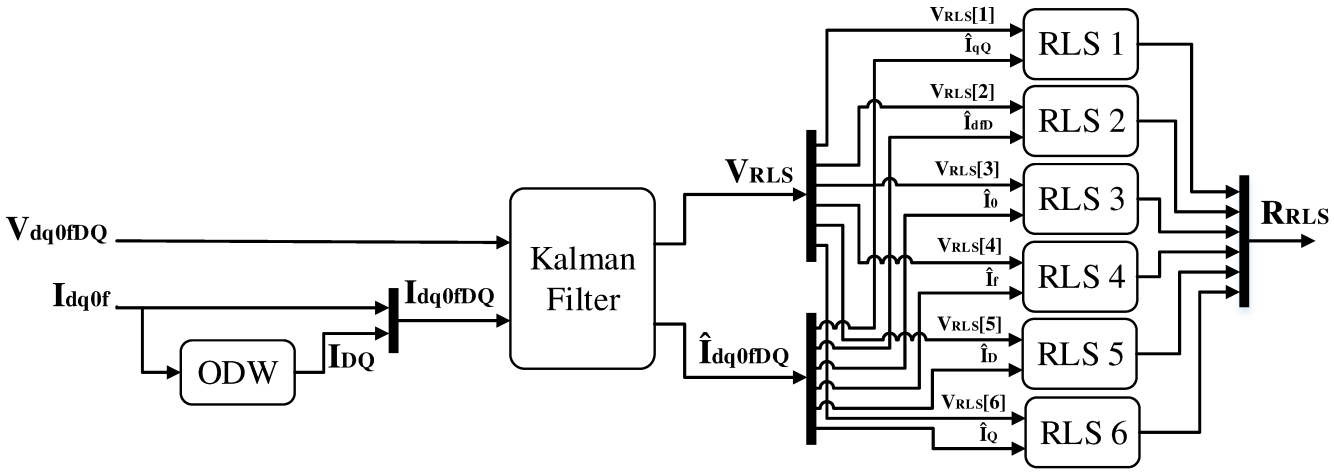

Fig. 4. Overview of the proposed parameter identification procedure

The output of the KF is fed into six RLS estimators, i.e. one for each line of $\mathbf{R_{RLS}}$, as seen in fig. 4. The estimators use a memory time of 3 seconds and sampling frequency of 400 Hz. Results are evaluated measuring the error in percentage from values in table I.

Table IV present a summary of these evaluations. Results are shown before and after the AVR step in order to demonstrate the effectiveness of the steady-state detection and robustness of the procedure to transient effects. Below follow some remarks about these results:

- The proposed procedure estimates parameters of the SPS SM machine with relative small percentage deviations, whose values are in line with those reported in the literature [16];
- The low standard deviation between all cases indicates the estimation is not sensitive to the load connected to the machine;
- Noise power has small influence in the quality of the parameter estimation;
- The strategy to disable and reset the RLS algorithm during transients is successful, as results are similar before and after the AVR step. No instability is observed in the estimated parameters for all cases and noise scenarios, also for long time simulations of 300 seconds in all noise scenarios (not included in the results for sake of brevity);
- The error of $\omega L_d, \omega L_{ad}$ estimations is considerable due to the saturation effect. However, there is no direct correlation between the amplitude of this deviation and the saturation level, as one would expect. This fact is clearly seen in case 3, which has the largest errors, but the smallest field current from all cases.
- Noise power continues to have small influence on the quality of the parameter estimation even with errors in the model caused by saturation. This seems to be an advantage of the KF over other filtering techniques reported in the literature [15], [16], but must be corroborated with experimental results.

V. Discussions and conclusions

The focus of this paper was the investigation and implementation of a procedure for reliable parameter identification for salient pole synchronous machines that can be used for condition monitoring, online assessment of the power grid, and adaptive control. Focus is given to a procedure that can: 1) run with the machine online, and without taking it out of service, performing difficult and time-consuming tests or involving large perturbations; 2) use common measurements available in a power plant without installing additional transducers in the machine; 3) be robust to noise and deviations in measurements caused by uncertainty of instruments or effects not included in the model.

In order to achieve that, a KF was implemented to filter and correct measurements using prior knowledge about the synchronous machine model and its parameters. Validation of the KF shows good correlation with the SM model available in SPS. The results also demonstrates the correlation is sensitive to saturation effects, but is insensitive to the load condition. The goodness of fit is maintained under a "standard" noise scenario. As one would expect, performance degrades in the "high" noise scenario, specially when the signal-to-noise ratio (SNR) is extremely low.

Outputs of the KF are then fed into a RLS algorithm that is able to reliably identify 8 out of 13 parameters from the SM: $R + 3R_N, R_f, R_D, R_Q, \omega L_d, \omega L_{ad}, \omega L_q, \omega L_{aq}$. The parameters not being estimated are: $R, L_0 + 3L_N, l_f, l_D, l_Q$, in which $R, L_0 + 3L_N$ are not relevant for calculation of standard parameters and the leakage reactances l_f, l_D, l_Q can be assumed as constants. Simulations show relatively small percentage deviations from the datasheet values, and are in line with those reported in the literature [16]. Besides, the estimator developed in this paper is largely insensitive to noise and load conditions, which may be considered a valuable contribution if corroborated with experimental results.

One limitation of this work is not including saturation effects in the model. Results show the KF effectively compen-

TABLE IV

PERCENTAGE ERRORS IN THE LAST 5 SECONDS OF ESTIMATION USING DATA SHEET VALUES AS BASELINE - BEFORE AND AFTER THE STEP

Param.	**Case 1**				**Case 2**				**Case 3**				**Case 4**			
	mean		**std dev**		**mean**		**std dev**		**mean**		**std dev**		**mean**		**std dev**	
	before	after	before	after	before	after	before	after	before	after	before	after	before	after	before	after
No noise scenario																
ωL_d	0.00	0.00	0.00	0.00	-1.63	-0.90	0.00	0.00	-4.04	-4.03	0.00	0.01	-3.26	-2.96	0.00	0.00
ωL_q	0.26	-0.01	0.00	0.00	-0.87	-0.97	0.03	0.01	-0.22	-0.26	0.01	0.00	-0.79	-0.85	0.02	0.00
$R + 3R_N$	0.00	0.00	0.00	0.00	0.00	0.00	0.00	0.00	0.00	0.00	0.00	0.00	0.00	0.00	0.00	0.00
ωL_{ad}	-0.08	-3.51	0.01	0.01	3.26	1.84	0.00	0.00	5.17	5.17	0.01	0.01	5.20	4.76	0.00	0.00
R_f	0.52	0.02	0.10	0.00	0.00	-0.04	0.00	0.01	0.00	-0.33	0.00	0.09	0.00	-0.07	0.00	0.02
R_D	-0.01	0.00	0.00	0.00	0.00	0.00	0.00	0.00	0.00	0.00	0.00	0.00	0.00	0.00	0.00	0.00
ωL_{aq}	0.02	0.00	0.00	0.00	-0.02	0.00	0.00	0.00	-0.02	0.00	0.00	0.00	-0.02	0.00	0.00	0.00
R_Q	0.00	0.00	0.00	0.00	-0.02	-0.02	0.00	0.00	-0.02	0.00	0.00	0.00	-0.02	-0.01	0.00	0.00
T'_{d0}	-0.54	-1.65	0.10	0.00	1.51	0.89	0.00	0.01	2.40	2.73	0.00	0.08	2.41	2.28	0.00	0.02
T'_d	-0.34	-0.05	0.10	0.00	-0.61	-0.66	0.02	0.02	-0.12	0.17	0.01	0.09	-0.53	-0.53	0.01	0.02
T''_{d0}	-0.03	-1.60	0.00	0.00	1.44	0.82	0.00	0.00	2.27	2.28	0.00	0.00	2.28	2.09	0.00	0.00
T''_d	1.01	-0.16	0.02	0.01	-3.63	-4.19	0.13	0.04	-0.69	-0.96	0.04	0.00	-3.20	-3.57	0.07	0.02
X'_d	0.35	-1.65	0.01	0.01	0.03	-0.81	0.05	0.02	1.98	1.88	0.01	0.00	1.03	0.70	0.03	0.01
X''_d	1.41	-0.22	0.02	0.02	-4.97	-5.74	0.18	0.06	-0.97	-1.34	0.06	0.00	-4.39	-4.89	0.10	0.02
T''_{q0}	0.02	0.00	0.00	0.00	0.01	0.02	0.00	0.00	0.01	0.00	0.00	0.00	0.01	0.01	0.00	0.00
X''_q	0.64	-0.03	0.01	0.01	-2.32	-2.63	0.08	0.03	-0.54	-0.70	0.03	0.00	-2.09	-2.30	0.05	0.01
Standard noise scenario																
ωL_d	-0.02	-0.01	0.00	0.00	-1.64	-0.91	0.00	0.00	-4.04	-4.04	0.00	0.01	-3.26	-2.97	0.00	0.00
ωL_q	0.22	-0.02	0.01	0.01	-0.88	-0.97	0.03	0.01	-0.22	-0.26	0.01	0.00	-0.79	-0.85	0.02	0.00
$R + 3R_N$	-0.06	-0.04	0.06	0.03	-0.02	-0.03	0.04	0.03	-0.02	-0.03	0.04	0.03	-0.02	-0.03	0.04	0.03
ωL_{ad}	-0.08	-3.51	0.01	0.01	3.25	1.84	0.00	0.00	5.17	5.17	0.00	0.01	5.20	4.76	0.00	0.00
R_f	0.41	0.12	0.08	0.02	-0.03	0.01	0.01	0.01	-0.08	-0.22	0.02	0.09	-0.03	-0.03	0.01	0.02
R_D	-0.03	-0.01	0.00	0.00	-0.01	-0.01	0.00	0.00	-0.01	-0.02	0.00	0.00	-0.01	-0.01	0.00	0.00
ωL_{aq}	0.03	0.00	0.00	0.00	-0.01	0.01	0.00	0.00	-0.01	0.01	0.00	0.00	0.00	0.01	0.00	0.00
R_Q	-0.01	0.00	0.00	0.00	-0.03	-0.02	0.00	0.00	-0.03	-0.01	0.00	0.00	-0.03	-0.02	0.00	0.00
T'_{d0}	-0.43	-1.74	0.08	0.02	1.54	0.85	0.01	0.01	2.48	2.62	0.02	0.09	2.44	2.23	0.01	0.02
T'_d	-0.27	-0.15	0.08	0.02	-0.58	-0.71	0.03	0.02	-0.04	0.05	0.03	0.09	-0.52	-0.58	0.02	0.02
T''_{d0}	-0.02	-1.59	0.00	0.00	1.45	0.83	0.00	0.00	2.28	2.29	0.00	0.00	2.29	2.10	0.00	0.00
T''_d	0.85	-0.22	0.04	0.02	-3.68	-4.21	0.14	0.04	-0.71	-0.96	0.05	0.00	-3.27	-3.61	0.09	0.02
X'_d	0.29	-1.68	0.02	0.01	0.00	-0.82	0.06	0.02	1.97	1.87	0.02	0.00	0.99	0.68	0.03	0.01
X''_d	1.15	-0.31	0.06	0.04	-5.06	-5.78	0.20	0.06	-1.01	-1.36	0.07	0.01	-4.50	-4.95	0.12	0.03
T''_{q0}	0.03	0.01	0.00	0.00	0.02	0.03	0.00	0.00	0.02	0.01	0.00	0.00	0.03	0.03	0.00	0.00
X''_q	0.53	-0.07	0.02	0.02	-2.35	-2.65	0.09	0.03	-0.56	-0.71	0.03	0.00	-2.13	-2.32	0.05	0.01
High noise scenario																
ωL_d	-0.19	-0.11	0.04	0.03	-1.70	-0.97	0.02	0.02	-4.08	-4.06	0.01	0.01	-3.31	-3.01	0.01	0.01
ωL_q	0.01	-0.13	0.05	0.03	-0.91	-0.97	0.03	0.01	-0.22	-0.25	0.01	0.00	-0.81	-0.85	0.02	0.00
$R + 3R_N$	-0.62	-0.39	0.56	0.34	-0.16	-0.31	0.41	0.33	-0.16	-0.34	0.41	0.33	-0.23	-0.33	0.41	0.32
ωL_{ad}	-0.07	-3.50	0.01	0.01	3.22	1.81	0.01	0.01	5.15	5.15	0.00	0.00	5.17	4.73	0.01	0.01
R_f	0.24	0.32	0.06	0.06	-0.11	0.11	0.03	0.03	-0.27	0.03	0.08	0.11	-0.09	0.06	0.03	0.03
R_D	-0.18	-0.09	0.03	0.02	-0.11	-0.09	0.02	0.02	-0.13	-0.11	0.03	0.03	-0.12	-0.09	0.02	0.02
ωL_{aq}	0.11	0.04	0.01	0.01	0.11	0.11	0.03	0.03	0.05	0.05	0.01	0.01	0.15	0.13	0.03	0.03
R_Q	-0.06	-0.03	0.01	0.01	-0.08	-0.07	0.01	0.01	-0.07	-0.04	0.01	0.01	-0.10	-0.08	0.02	0.02
T'_{d0}	-0.26	-1.93	0.06	0.05	1.61	0.74	0.04	0.03	2.67	2.37	0.08	0.11	2.49	2.14	0.03	0.03
T'_d	-0.30	-0.46	0.04	0.05	-0.61	-0.87	0.07	0.04	0.10	-0.22	0.09	0.12	-0.58	-0.75	0.06	0.05
T''_{d0}	0.14	-1.51	0.03	0.02	1.54	0.89	0.02	0.02	2.40	2.37	0.03	0.03	2.38	2.17	0.02	0.02
T''_d	-0.22	-0.74	0.22	0.15	-4.21	-4.52	0.22	0.11	-0.87	-1.05	0.07	0.02	-3.90	-4.01	0.19	0.11
X'_d	-0.19	-1.92	0.10	0.07	-0.25	-0.98	0.10	0.05	1.85	1.79	0.04	0.02	0.71	0.48	0.08	0.06
X''_d	-0.55	-1.16	0.35	0.24	-5.89	-6.30	0.33	0.17	-1.40	-1.61	0.14	0.07	-5.47	-5.59	0.28	0.18
T''_{q0}	0.13	0.06	0.02	0.01	0.16	0.14	0.03	0.03	0.10	0.08	0.02	0.02	0.20	0.17	0.04	0.04
X''_q	-0.22	-0.44	0.15	0.11	-2.70	-2.86	0.14	0.07	-0.72	-0.81	0.06	0.03	-2.54	-2.59	0.12	0.08

sates saturation for v_q, i_f. However, saturation considerably affects the estimation error of ωL_{ad} and the measurement of i_D provided by the ODW, whose zeros and poles are directly affected by L_{ad}. Surprisingly, there is no direct correlation between the amplitude of this deviation and the saturation level. This fact that is clearly seen in results of case 3, which has the largest errors for $\omega L_d, \omega L_{ad}$, but the lowest saturation level.

Therefore, saturation effects must be considered and included in future work. An alternative for that would be using an extended or unscented KF, which can handle non linear state transition functions, and compensate the value of L_{ad} dynamically [19]. Alternatively, a more advanced non linear model of the machine including saturation in its derivation can be used [33], [34].

Despite current limitations, results are promising and, when validated experimentally, the proposed procedure can already be used for practical condition monitoring applications, such as detection of broken damper winding, turn-to-turn short circuit and air-gap eccentricity. Another possibility is using the proposed procedure to calculate standard parameters in multiple load conditions based on measurements from existing protection IEDs, without the use of special test equipment.

REFERENCES

[1] NVE, "Vannkraftpotensialet," https://www.nve.no/energiforsyning-og-konsesjon/vannkraft/vannkraftpotensialet/, Dec. 2017.

[2] P. Kundur, N. J. Balu, and M. G. Lauby, *Power System Stability and Control*, ser. The EPRI Power System Engineering Series. New York: McGraw-Hill, 1994.

[3] I. M. Canay, "Causes of Discrepancies on Calculation of Rotor Quantities and Exact Equivalent Diagrams of the Synchronous Machine," *IEEE Trans. Power Appar. Syst.*, vol. PAS-88, no. 7, pp. 1114–1120, Jul. 1969.

[4] W. Jackson and R. Winchester, "Direct- and Quadrature-Axis Equivalent Circuits for Solid-Rotor Turbine Generators," *IEEE Trans. Power Appar. Syst.*, vol. PAS-88, no. 7, pp. 1121–1136, Jul. 1969.

[5] N. Bianchi, *Electrical Machine Analysis Using Finite Elements*, ser. Power Electronics and Applications Series. Boca Raton, FL: Talor & Francis, 2005, oCLC: ocm57694820.

[6] J. Lidenholm and U. Lundin, "Estimation of Hydropower Generator Parameters Through Field Simulations of Standard Tests," *IEEE Trans. Energy Convers.*, vol. 25, no. 4, pp. 931–939, Dec. 2010.

[7] IEEE, *Std 115-2009 IEEE Guide for Test Procedures for Synchronous Machines*. New York: IEEE, May 2010, oCLC: 958760789.

[8] IEC, *IEC 60034-4 Rotating Electrical Machines – Part 4: Methods for Determining Synchronous Machine Quantities from Tests*, 3rd ed. IEC, May 2008.

[9] G. Dajaku and D. Gerling, "Air-Gap Flux Density Characteristics of Salient Pole Synchronous Permanent-Magnet Machines," *IEEE Trans. Magn.*, vol. 48, no. 7, pp. 2196–2204, Jul. 2012.

[10] F. P. de Mello and L. N. Hannett, "Representation of Saturation in Synchronous Machines," *IEEE Trans. Power Syst.*, vol. 1, no. 4, pp. 8–14, 1986.

[11] Statnett, "Funksjonskrav i kraftsystemet," 2012.

[12] L. Ljung, "Lennart Ljung on System Identification Toolbox: History and Development - Video," https://www.mathworks.com/videos/lennart-ljung-on-system-identification-toolbox-history-and-development-96989.html, Apr. 2012.

[13] J. Verbeeck, R. Pintelon, and P. Lataire, "Influence of saturation on estimated synchronous machine parameters in standstill frequency response tests," *IEEE Trans. Energy Convers.*, vol. 15, no. 3, pp. 277–283, Sept./2000.

[14] E. Bortoni and J. Jardini, "Identification of synchronous machine parameters using load rejection test data," *IEEE Trans. Energy Convers.*, vol. 17, no. 2, pp. 242–247, Jun. 2002.

[15] H. Karayaka, A. Keyhani, G. Heydt, B. Agrawal, and D. Selin, "Synchronous generator model identification and parameter estimation from operating data," *IEEE Trans. Energy Convers.*, vol. 18, no. 1, pp. 121–126, Mar. 2003.

[16] E. Kyriakides, G. Heydt, and V. Vittal, "Online Parameter Estimation of Round Rotor Synchronous Generators Including Magnetic Saturation," *IEEE Trans. Energy Convers.*, vol. 20, no. 3, pp. 529–537, Sep. 2005.

[17] M. Dehghani and S. Nikravesh, "Nonlinear state space model identification of synchronous generators," *Electr. Power Syst. Res.*, vol. 78, no. 5, pp. 926–940, May 2008.

[18] M. A. Arjona, M. Cisneros-Gonzalez, and C. Hernandez, "Parameter Estimation of a Synchronous Generator Using a Sine Cardinal Perturbation and Mixed Stochastic–Deterministic Algorithms," *IEEE Trans. Ind. Electron.*, vol. 58, no. 2, pp. 486–493, Feb. 2011.

[19] E. Ghahremani and I. Kamwa, "Online State Estimation of a Synchronous Generator Using Unscented Kalman Filter From Phasor Measurements Units," *IEEE Trans. Energy Convers.*, vol. 26, no. 4, pp. 1099–1108, Dec. 2011.

[20] M. Cisneros-González, C. Hernandez, R. Morales-Caporal, E. Bonilla-Huerta, and M. A. Arjona, "Parameter Estimation of a Synchronous-Generator Two-Axis Model Based on the Standstill Chirp Test," *IEEE Trans. Energy Convers.*, vol. 28, no. 1, pp. 44–51, Mar. 2013.

[21] J. Bladh, M. Wallin, L. Saarinen, and U. Lundin, "Standstill Frequency Response Test on a Synchronous Machine Extended With Damper Bar Measurements," *IEEE Trans. Energy Convers.*, vol. 31, no. 1, pp. 46–56, Mar. 2016.

[22] B. Zaker, G. B. Gharehpetian, M. Karrari, and N. Moaddabi, "Simultaneous Parameter Identification of Synchronous Generator and Excitation System Using Online Measurements," *IEEE Trans. Smart Grid*, vol. 7, no. 3, pp. 1230–1238, May 2016.

[23] A. Belqorchi, U. Karaagac, J. Mahseredjian, and I. Kamwa, "Standstill Frequency Response Test and Validation of a Large Hydrogenerator," *IEEE Trans. Power Syst.*, vol. 34, no. 3, pp. 2261–2269, May 2019.

[24] J. Machowski, J. W. Bialek, and J. R. Bumby, *Power System Dynamics: Stability and Control*, 2nd ed. Chichester, U.K: Wiley, 2008, oCLC: ocn232130756.

[25] C. R. IEEE, "Recommended Phasor Diagram for Synchronous Machines," *IEEE Trans. Power Appar. Syst.*, vol. PAS-88, no. 11, pp. 1593–1610, 1969.

[26] T. A. Lipo, "A Cartesian Vector Approach To Reference Theory of AC Machine," Wiscosin Electric Machines and Power Electronics Consortium, Madison, Wisconsin, Reseach Report 84-2, Apr. 1984.

[27] E. Clarke, *Circuit Analysis of A-C Power Systems; Symmetrical and Related Components.*, ser. General Electric Series. New York: Wiley, 1943.

[28] A. Barakat, S. Tnani, G. Champenois, and E. Mouni, "Analysis of synchronous machine modeling for simulation and industrial applications," *Simul. Model. Pract. Theory*, vol. 18, no. 9, pp. 1382–1396, Oct. 2010.

[29] T. Glad and L. Ljung, *Control Theory: Multivariable and Nonlinear Methods*. London: Taylor & Francis, 2000, oCLC: 247761966.

[30] IEEE, *421.5-2016 - IEEE Recommended Practice for Excitation System Models for Power System Stability Studies*, 2016th ed., ser. IEEE 421. New York: IEEE, Aug. 2016, no. 5.

[31] M. Namba, T. Nishiwaki, S. Yokokawa, K. Ohtsuka, and Y. Ueki, "Identification of Parameters for Power System Stability Analysis Using Kalman Filter," *IEEE Power Eng. Rev.*, vol. PER-1, no. 7, pp. 37–37, Jul. 1981.

[32] L. Ljung, *System Identification: Theory for the User*, 2nd ed., ser. Prentice Hall Information and System Sciences Series. Upper Saddle River, NJ: Prentice Hall PTR, 1999.

[33] E. Levi, "State-space d–q axis models of saturated salient pole synchronous machines," *IEE Proc. - Electr. Power Appl.*, vol. 145, no. 3, p. 206, 1998.

[34] H. Rehaoulia, H. Henao, and G. Capolino, "Modeling of synchronous machines with magnetic saturation," *Electr. Power Syst. Res.*, vol. 77, no. 5-6, pp. 652–659, Apr. 2007.